DYNAMICS AND CHEMISTRY OF MARINE STRATOCUMULUS—DYCOMS-II

BY BJORN STEVENS, DONALD H. LENSCHOW, GABOR VALI, HERMANN GERBER, A. BANDY, B. BLOMQUIST, J.-L. BRENGUIER, C. S. BRETHERTON, F. BURNET, T. CAMPOS, S. CHAI, I. FALOONA, D. FRIESEN, S. HAIMOV, K. LAURSEN, D. K. LILLY, S. M. LOEHRER, SZYMON P. MALINOWSKI, B. MORLEY, M. D. PETTERS, D. C. ROGERS, L. RUSSELL, V. SAVIC-JOVCIC, J. R. SNIDER, D. STRAUB, MARCIN J. SZUMOWSKI, H. TAKAGI, D. C. THORNTON, M. TSCHUDI, C. TWOHY, M. WETZEL, AND M. C. VAN ZANTEN

Measurements in marine stratocumulus over the northeast Pacific help scientists unravel the mysteries of this important cloud regime.

The stratocumulus-topped boundary layer (hereafter the STBL), which prevails in the subtropics in regions where the underlying ocean is much colder than the overlying atmosphere, is thought to be an important component of the climate system. Perhaps most striking is its impact on the radiative balance at the top of the atmosphere. The seasonally averaged net cloud radiative forcing from the STBL has been estimated to be as large as 70 W m^{-2} (Stephens and Greenwald 1991), more than an order of magnitude larger than the radiative forcing associated with a doubling of atmospheric CO_2. This means that even rather subtle sensitivities of the STBL to changes in the properties of the atmospheric aero-

AFFILIATIONS: STEVENS, SAVIC-JOVCIC, AND VAN ZANTEN,—Department of Atmospheric Sciences, University of California, Los Angeles, Los Angeles, California; LENSCHOW, CAMPOS, FALOONA, FRIESEN, LAURSEN, MORLEY, ROGERS, AND TSCHUDI—National Center for Atmospheric Research, Boulder, Colorado; VALI, HAIMOV, PETTERS, SNIDER, AND TAKAGI—Department of Atmospheric Science, University of Wyoming, Laramie, Wyoming; GERBER—Gerber Scientific Inc., Reston, Virginia; BANDY, BLOMQUIST, AND THORNTON—Department of Chemistry, Drexel University, Philadelphia, Pennsylvania; BRENGUIER AND BURNET—CNRM Météo-France, Toulouse, France; BRETHERTON—Department of Atmospheric Sciences, University of Washington, Seattle, Washington; CHAI, SZUMOWSKI, AND WETZEL—Desert Research Institute, Reno, Nevada; LILLY—School of Meteorology, University of Oklahoma, Norman, Oklahoma; LOEHRER—Joint Office for Science Support, University Corporation for Atmospheric Research, Boulder, Colorado; MALINOWSKI—Institute of Geophysics, Warsaw University, Warsaw, Poland; RUSSELL—Princeton University, Princeton, New Jersey; STRAUB—Department of Atmospheric Science, Colorado State University, Fort Collins, Colorado; TWOHY—College of Oceanography and Atmospheric Sciences, Oregon State University, Corvallis, Oregon

A supplement to this article is available online (DOI: 10.1175/BAMS-84-5-Stevens)

CORRESPONDING AUTHOR: Bjorn Stevens, Dept. of Atmospheric Sciences, University of California, Los Angeles, 405 Hilgard Ave., Box 951565, Los Angeles, CA 90095-1565
E-mail: bstevens@atmos.ucla.edu

DOI: 10.1175/BAMS-84-5-579

In final form 26 December 2002

sol (cf. Twomey 1974; Albrecht 1989; Brenguier et al. 2000b), or the large-scale environment (Rodwell and Hoskins 2001), can still project significantly onto the overall radiative budget. In addition, the effect of the STBL on the surface energy budget and thus the overall climatology of the Tropics is also thought to be significant (cf. Mechoso et al. 1995; Ma et al. 1996; Philander et al. 1996). However, attempts to quantify these, and other, effects are frustrated by our inability to quantify, let alone understand, key elements of stratocumulus physics.

Two questions stand out: First, how efficiently do stratocumulus entrain (incorporate through turbulent mixing) air from the warm, dry, quasi-laminar, free troposphere into the cool, moist, turbulent boundary layer? Second, how important is drizzle? The two processes are, of course, related. Both act directly to reduce the amount of water in the cloud layer, and indirectly to modify the heat budget, thereby impacting the dynamics. Moreover, because drizzle is thought to suppress entrainment (Stevens et al. 1998), and because entrainment is thought to suppress drizzle, the interplay between the processes may be subtle, which could make them difficult to untangle. Nonetheless, recent advances in observational technology have introduced new possibilities for understanding entrainment, drizzle, and external processes (such as factors regulating cloud microstructure, and cloud–aerosol interactions), which may regulate this interplay. This combination of refined theoretical questions, and advances in observational technologies, helped to motivate the second Dynamics and Chemistry of Marine Stratocumulus (DYCOMS-II) field study, which this paper aims to describe.

ENTRAINMENT. To help one understand why entrainment is so important it helps to think in terms of the mixed layer theory of Lilly (1968), wherein the STBL is identified as a distinct layer of the atmosphere whose properties are largely determined by exchanges with the underlying surface on the one hand, and dilution through the incorporation of air from the free troposphere (i.e., entrainment) on the other. The entrainment velocity, E can be defined in terms of an equation for the depth, h, of the STBL:

$$\frac{dh}{dt} = E + W_h, \tag{1}$$

where W_h is the large-scale vertical velocity evaluated at h. One can think of E as the diabatic growth rate of the layer. It essentially quantifies the dilution rate of the STBL and thus is critical in determining its overall state.

Interest in entrainment is not only motivated by its importance to the state of the STBL, but also by the extent to which previous work has been unable to constrain it. Indeed much recent work has been devoted toward articulating an entrainment rule, which given the mean state and the forcing would produce an estimate of E. Most of this work has been based on large eddy simulation. It has, in part, been spurred on by the startling results of Moeng et al. (1996), which show how simulations of the same case by different groups differ by nearly an order of magnitude in their prediction of the mixing (or entrainment) rate across cloud top. Such differences have subsequently been shown to be due to a variety of factors, most notably variability in the treatment of physical processes such as radiation and condensation. But numerical issues are also important, Stevens et al. (1999) show that insufficient resolution of the radiative cooling in the vicinity of the cloud-top interface leads to systematic biases in estimates of entrainment. More unified treatments of physical processes have helped reduce the discrepancies among models, but (perhaps because of poorly understood numerical sensitivities) significant differences persist. In a survey of recent work Stevens (2002) shows that different entrainment rules derived from state-of-the-art simulations can still differ by more than a factor of 2. Moreover, when these parameterizations are incorporated into a mixed-layer model, the equilibrium solutions for typical climatological conditions have equilibrium sensible and latent heat fluxes that vary by as much as 40 W m^{-2} and cloud liquid water paths that vary by factors of 2 or more. With this degree of discord, one might think that observations could usefully arbitrate disputes posed by models. However, estimating entrainment from real data has also proven to be challenging.

Fundamentally there are two different techniques for inferring E from data; we call these the divergence and tracer method, respectively. The divergence method evaluates E from (1) as

$$E = \frac{dh}{dt} + \int_0^h D\,dz, \tag{2}$$

where $D = \partial u/\partial x + \partial v/\partial y$ is the divergence of the horizontal wind. The tracer method evaluates E from the budget of trace constituents (denoted by c) across the cloud-top interfacial layer. If this layer is sufficiently

thin, and if sources of c are not important over this region, the budget requires that

$$E \approx \frac{(\overline{w'c'})h}{c_+ - \overline{c}}, \qquad (3)$$

where $(\overline{w'c'})_h$ is the turbulent flux just below the top of the cloud layer. The term in the denominator, often referred to as the jump and denoted Δc, measures the change in the constituent amount across the top of the STBL. Note that the number of independent estimates of E that can be deduced from the tracer method is only limited by ones ability to identify and measure tracers, c, with suitable properties, that is, well-defined jumps and negligible interfacial sources. Moreover, because $(\overline{w'c'})_h$ can be estimated independently in two ways (either directly via eddy correlation, or as a residual of the budget of c over the STBL as a whole), to the extent that the numerator in (3) is the source of uncertainty in the estimate of E, one can estimate E in two independent ways for each tracer.

In the past it has not been possible to estimate D from flight data in the STBL, and so investigators who have tried to use the divergence method, that is, (2), for estimating E have been forced to rely on forecast models for estimates of D (e.g., Bretherton et al. 1995; De Roode and Duynkerke 1997). As a consequence most previous estimates of E have been based on an application of the tracer method. For instance during DYCOMS-I (Lenschow et al. 1988) entrainment was estimated on the basis of fast response measurements of O_3 and H_2O (Kawa and Pearson 1989). Likewise, in his studies of stratocumulus over the North Sea, Nicholls (1984) estimated E based on the water budget. Subsequent studies (e.g., Bretherton et al. 1995; De Roode and Duynkerke 1997), have made similar estimates, either based on measurements of O_3 or water vapor. Despite the growing literature, previous observations have not provided particularly strong bounds on E. One reason is that neither H_2O nor O_3 are ideal tracers for estimating entrainment, so that estimates based on an application of the tracer method using these variables tend to have relatively large uncertainties. Another reason is that almost all observational estimates of entrainment have been for daytime, when the radiative forcing of the boundary layer is difficult to measure and changes considerably with time. In contrast, all of the theoretical work applies to nighttime, which eliminates these complications.

MORE ON ENTRAINMENT

To illustrate how entrainment helps regulate the state of the STBL we begin with the equation describing the evolution of the bulk (layer averaged) value of a horizontally homogeneous conserved scalar, c, in a marine layer of some depth h:

$$\frac{d\overline{c}}{dt} = \frac{(\overline{w'c'})_0 - (\overline{w'c'})_h}{h}. \qquad \textbf{(SB1)}$$

Here $(\overline{w'c'})_0$ is the flux of c evaluated at the surface, and $(\overline{w'c'})_h$ is the entrainment flux, that is, the turbulent flux of c estimated at the top of the layer. The surface flux $(\overline{w'c'})_0$ can be evaluated using similarity theory: $\overline{w'c'}_0 = C_d||\mathbf{U}||(c_s - \overline{c})$, where C_d is an exchange coefficient, c_s is the value of the scalar at the surface, and $\mathbf{U}$ is the vector wind (e.g., Deardorff 1972). If the entrainment zone is sufficiently thin, the entrainment flux can (in analogy to the surface flux) be linearly related to the entrainment velocity E: $(\overline{w'c'})_h = -E(c_+ - \overline{c})$ (e.g., Lilly 1968; Stevens 2002). Here c_+ is the value c takes just above the boundary layer. The depth of the layer h also depends on E following

$$\frac{dh}{dt} = E + W_h, \qquad \textbf{(SB2)}$$

with W_h being the large-scale vertical velocity evaluated at the top of the layer. If the divergence, D, of the mean horizontal wind is constant with height, then $W_h = -Dh$. In steady state the time derivatives in both (SB1) and (SB2) vanish leading to the following relations for the equilibrium values of $\overline{c}$ and h:

$$\overline{c} = \frac{C_d||U||c_s + Ec_+}{C_d||U|| + E} \quad \textbf{and} \quad h = \frac{E}{\langle D \rangle}. \qquad \textbf{(SB3)}$$

Here $\langle D \rangle$ denotes the bulk divergence within the boundary layer. Because boundary layer total-water specific humidity q_t and the liquid water static energy $s_l = c_pT + gz - Lq_l$ (the enthalpy variable) behave to a first approximation like conserved scalars, the above relations illustrate the critical role of E not only in determining the budgets of arbitrary scalars, but also in determining the mean thermodynamic state of the boundary layer and its depth. This latter information in turn determines other climatologically important quantities, such as cloud amount—or surface fluxes.

DYCOMS-II addressed these issues by sampling the clouds predominantly at night, and by attempting to estimate E using both the divergence and tracer methods. In addition to better constraints on the forcing, nighttime measurements eliminate solar forcing (which is difficult to measure) and thus facilitates estimates of the heat budget. Because the evolution of cloud base couples the heat and moisture budgets of the layer, simply tracking the evolution of cloud base during the night greatly constrains these budgets, thereby constraining heat or moisture budget based estimates of entrainment using (3).

During DYCOMS-II, tracer-based estimates of E were also based on measurements of two additional passive tracers, DMS (CH_3SCH_3 or dimethyl sulfide) and ozone (O_3). In these cases the numerator in (3) was estimated only from eddy correlation measurements, as budget residual estimates were more difficult to make. The use of DMS in this regard is novel. Because the only known source of DMS is at the surface, and because its lifetime (a few days) is too short to lead to appreciable concentrations in the free atmosphere but is long compared to the mixing timescale in the STBL, it should exhibit well-defined jumps. For this reason it is thought to be nearly ideal for estimating entrainment via (3). In contrast H_2O and O_3 can vary significantly above the boundary layer, leading to large uncertainties in estimates of the jumps, which frustrates the use of (3) to estimate E. Indeed O_3 sometimes has jumps that change sign across the study area (e.g., Kawa and Pearson 1989), thereby making the relation (3) ill defined. Another limitation of H_2O is that it is partitioned into two phases in the cloud layer; this makes it difficult to measure on the one hand, and introduces gravitational fluxes out of air parcels (drizzle), which behave in a nonconservative manner, on the other hand. DYCOMS-II hoped to at least overcome the measurement difficulties of H_2O in the cloud through the use of a new, high-rate, laser hygrometer [the TDL, or tunable diode laser; May (1998)] capable of making very precise measurements of water vapor in cloud. Although in principle DMS has more potential as a means for estimating entrainment, the idea was not to supplant the other tracer-based methods of estimating E, but rather to supplement them with an additional tracer-based method of comparable or greater accuracy.

DYCOMS-II also was designed around the possibility of estimating E using the divergence method. To do so requires a means for estimating D, and the evolution of h. Technological advancements that make this feasible include the development of the scanning

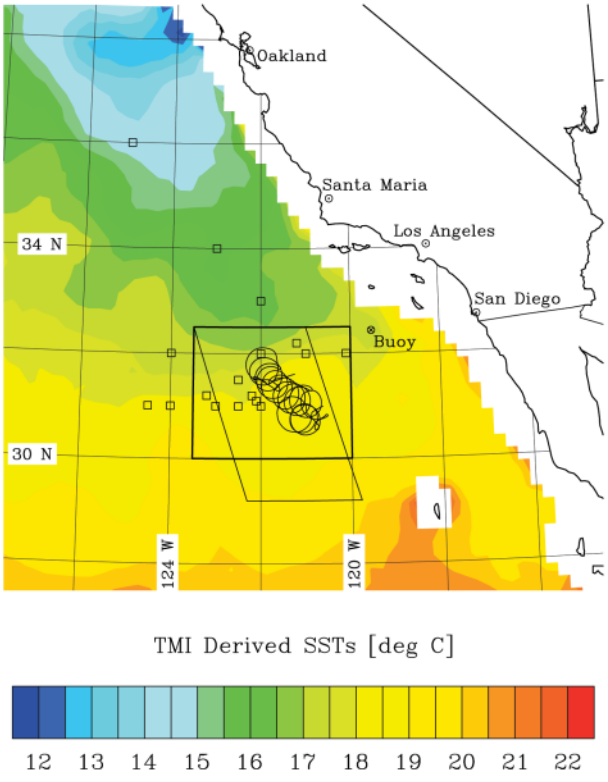

Fig. 1. DYCOMS-II target area superimposed on TMI-derived SSTs for the experimental period [the Tropical Rainfall Measurement Mission (TRMM) Microwave Imager (TMI), sees through nonprecipitating cloud decks]. The planned target area (for which forecast data are archived) is shown by the rectangle. The actual target area, where 90%–95% of the measurements were made (excluding ferries), is shown by the rhomboid. Flight track RF07 is also overlaid to illustrate a typical entrainment flight pattern. Open boxes are approximate locations of previous flights during DYCOMS-I and 8 of the 10 FIRE flights. The location of the Tanner Banks buoy is also noted.

aerosol backscatter lidar (SABL) and the GPS-corrected wind fields. The SABL gives precise measurements of cloud-top height when flying above cloud. GPS corrections to the gust probe plus inertial reference system estimates of the wind motivate estimates of D by integrating the track-normal component of the lateral velocity field around a closed flight track (Lenschow 1996; Lenschow et al. 1999). The mean vertical velocity at the STBL top may then be estimated as $-Dh$. In addition, proxy data from forecast models, and estimates of D directly from remotely sensed wind fields (e.g., SeaWinds; Liu 2002), and the tracking of layers in composite soundings from dropsondes, all provide additional constraints and bounds on the method, thereby increasing our ability to evaluate E from (2).

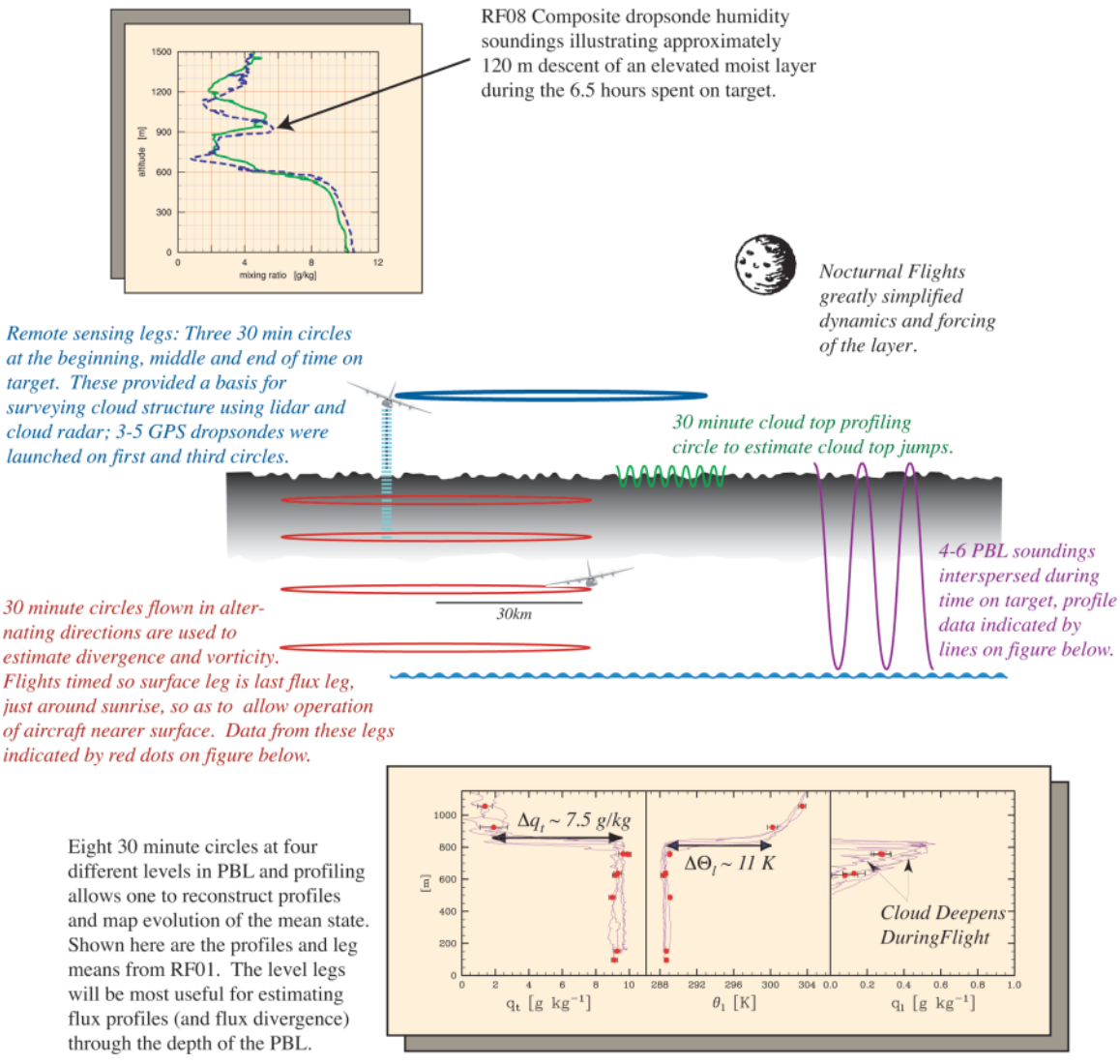

FIG. 2. DYCOMS-II flight strategy. Symbols in bottom panel refer to total water mixing ratio q_t; its change across cloud top, Δq_t; liquid water potential temperature, θ_l; its change across cloud top, $\Delta\theta_l$; and liquid water mixing ratio q_l.

One last technological development that motivated a new observational attack on the entrainment problem was the availability of the National Science Foundation/National Center for Atmospheric Research (NSF/NCAR) C130. Its long range facilitates more extensive sampling of more remote layers, and its large payload enables the delivery of a greater range of scientific instrumentation to the target area.

THE FLIGHTS. The field program took place in July 2001. Remotely sensed data, forecast model output, and other data of opportunity were collected and archived for the entire month, and research flights took place from 7 to 28 July 2001. Flight operations were based out of North Island Naval Air Station, just across the bay from San Diego. The target area was approximately 1 h west southwest of San Diego as illustrated in Fig. 1. The field program consisted of seven entrainment research flights and two radar research flights.

The entrainment flights were designed following a template illustrated with the aid of Fig. 2. Although no single flight followed this schematic exactly, its essential elements were incorporated into every entrainment flight. These elements included circles to estimate divergences and fluxes concurrently (see also the flight track in Fig. 1) and long legs to reduce sampling errors in fluxes and other higher-order statistics. The stacking of these legs can allow better estimates of cloud-top or surface fluxes. In addition, frequent profiling of the layer facilitated evaluation of the layer

evolution. Last, the long legs above cloud allowed ample time for remote sampling of the layer.

Experimental conditions during DYCOMS-II were excellent. The uniformity and extent of cloud cover were unprecedented, even for stratocumulus experiments. An example of the morning satellite imagery for RF01 is given in Fig. 3; if anything, the areal extent of the cloud layer was less on this flight than on subsequent flights. We attribute the favorable conditions to two factors: First, seven of nine research flights were nocturnal, and satellite images often showed that daytime gaps in the cloud layer tended to fill during the early evening—well before our usual takeoff time of around 2315 local time. Second, the synoptic environment was more conducive to well-formed stratocumulus than usual. In past experiments it has been customary to rank cases, based on uniformity of cloud cover. For instance during DYCOMS-II Lenschow et al. (1988) developed a seven-point scale for rating cloud cover, with one denoting solid, unbroken stratus, two near solid, with occasional breaks, and three to seven denoting increasingly broken or more variable boundary layers. Although DYCOMS-I experienced generally more ideal conditions than subsequent large experiments (e.g., Albrecht et al. 1988, 1995) only one of the DYCOMS-I flights rated a one on the Lenschow scale, with three other flights rating a two. In contrast eight of the nine DYCOMS-II flights rated a one. The lone deviant was RF02, which had only 97% lidar-derived cloud cover and thus rated a two.

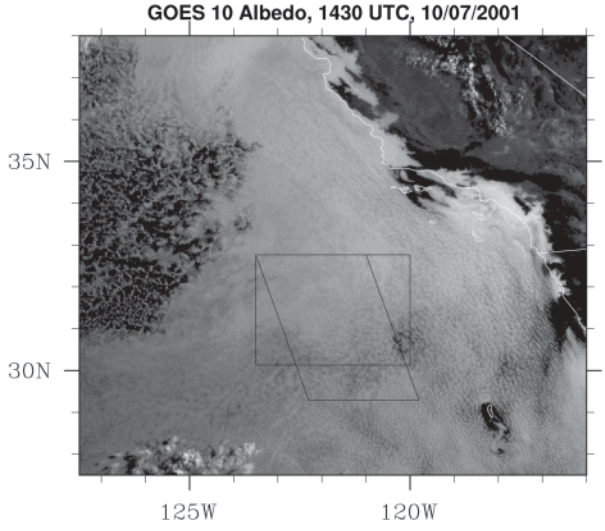

Fig. 3. *GOES-10* channel 1 (visible) image for conditions near the end of RF01. Note widespread region of uniform marine stratocumulus cloud cover surrounding the target area. The preliminary target area is boxed; the actual region in which almost all of the flight hours were spent is bounded by the rhomboid.

Apart from the uniformity of cloud cover, the structure of observed cloud layers varied greatly. Boundary layer depths varied by nearly a factor of 2 (from lows of 600 m on several of the flights to a high of 1100 m on RF04). Cloud depths, and cloud-top liquid water concentrations varied similarly, with cloud depths ranging from less than 300 to over 500 m and liquid water concentrations from 0.5 to 1.0 g kg^{-1}. In contrast, DYCOMS-I also experienced relatively well-formed stratus layers, but the cloud depths were thinner, between 100 and 300 m. Surface winds during DYCOMS-II were generally northwesterly but their magnitude varied considerably, from 5 to 12 m s^{-1}. Microphysically we also observed rich differences in cloud structure, with some cloud layers having small numbers of cloud droplets, characteristic of a pristine marine environment, and others having somewhat larger concentrations of cloud droplets, indicative of a greater continental influence. Drizzle was common, with some flights showing persistent radar echos greater than 20 dB*Z*. Further details and a more quantitative overview of the flights are provided in the electronic supplement to this article (DOI: 10.1175/BAMS-84-5-Stevens). The variety of conditions sampled should enable an evaluation of how different aspects of the mean state influence the dynamics and physics of the cloud layer.

Much of the variability in cloud conditions correlates with variations in synoptic conditions. During the second week of flight operations (corresponding to research flights 4–6), the Pacific high strengthened and its major axis became oriented along a more north–south direction. At the same time a strong low pressure system developed off the coast of British Columbia, centered over Seattle at 0000 UTC on 17 July. The influence of this depression was felt over the target area at upper levels and was associated with strong cold-air advection aloft. The 850-hPa temperature decreased by 8 K through the month and by 4 K through the first week of the experiment. These changes resulted in significantly weaker inversions and generally deeper (800–1100 m) boundary layers with more variability in cloud-top height through the course of a given mission.

Large flight-to-flight variability is also apparent in DMS concentrations (Fig. 4). DMS is rather more dilute when the boundary layer is deep (RF04 and RF05) and rather more concentrated when the boundary layer is shallow (RF03). Unlike some other tracers, DMS also varied considerably within a flight. As we had hoped, DMS existed in ample amounts on

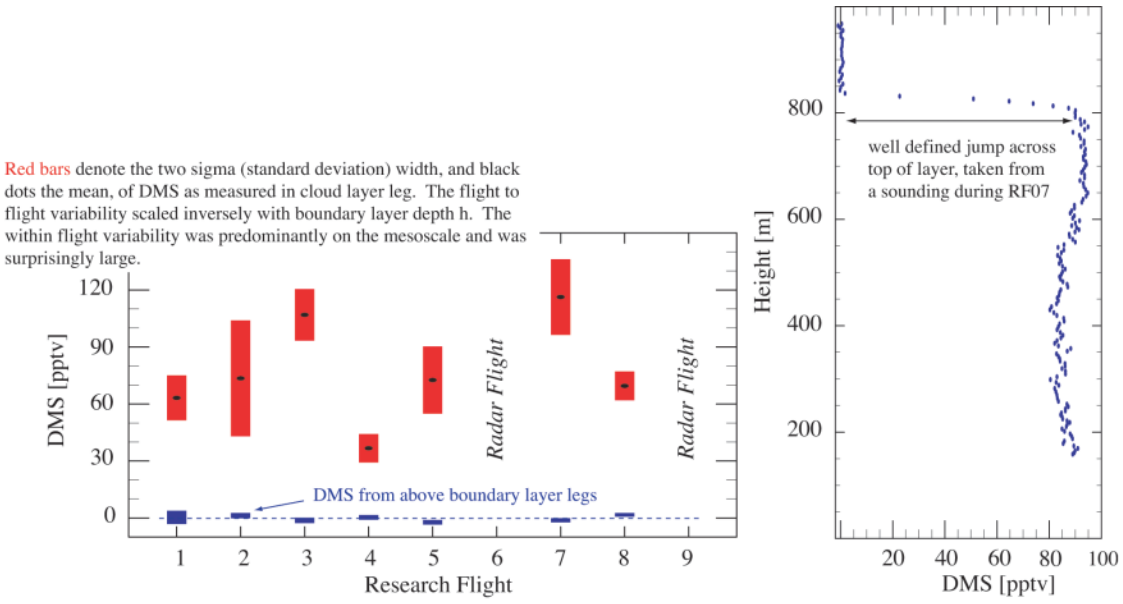

FIG. 4. DMS concentrations from entrainment flights.

every leg within the STBL, but was effectively absent above, leading to well-defined jumps locally. However we were surprised to routinely see DMS variations exceeding 20% around flight circles in the STBL. The origin of pronounced variability remains a mystery.

DRIZZLE. Few dispute that in regions where drizzle occurs, it is a key component of the water budget and can have an important impact on the dynamics and structure of the STBL. However, its role in the climatology of clouds on larger scales is controversial. Previous field programs have suggested that drizzle might be a relatively common phenomenon (e.g., Brost et al. 1982; Duynkerke et al. 1995; Fox and Illingworth 1997; Vali et al. 1998) and, thus, could play a vital role in the evolution of the STBL (e.g., Paluch and Lenschow 1991). In this respect simple theoretical models (e.g., Albrecht 1989; Ackerman et al. 1993; Wang and Albrecht 1986; Pincus and Baker 1994) suggest that the modulation of drizzle by changes in the atmospheric aerosol could regulate cloud amount and thickness. Because these ideas provide a straightforward mechanism whereby human activity could affect cloudiness, they have attracted considerable attention. Although there exists a modest and growing literature on drizzle in the STBL (e.g., Chen and Cotton 1987; Wang and Wang 1994; Austin et al. 1995; Gerber 1996; Stevens et al. 1998; Vali et al. 1998) some very elementary questions remain, including the actual precipitation rates in marine stratocumulus and their relation to ambient aerosol, cloud thickness, and intensity of turbulence. For this reason, a central element of the DYCOMS-II was an evaluation of drizzle processes in stratocumulus.

The tendency toward less drizzle during the daytime, evidence of large spatial and temporal variability, and suggestions of considerable vertical structure have all frustrated attempts to quantify its role. In the past these problems were compounded by an exclusive reliance on in situ probes, whose sampling statistics are poor and whose measurements, because of the intermingling of spatial and temporal variability, are difficult to interpret. Cloud radars, on the other hand, sample much larger volumes, can rapidly profile an entire column (or layer depending on their orientation), and are sensitive to larger moments of the droplet spectrum. Thus they seem like a natural way to study drizzle. For this reason the University of Wyoming Cloud Radar (WCR) was mounted on the NSF/NCAR C130 for DYCOMS-II.

The WCR was mounted in the rear of the aircraft and alternately looked through two antennas, one that pointed straight down, and one that looked down and rearward (see electronic supplement DOI: 10.1175/BAMS-84-5-Stevens). The DYCOMS-II flight strategy, with cloud and subcloud legs, allows comparison of in situ microphysical probe data with the radar reflectivity data from just below the aircraft to calibrate reflectivity–rain-rate relationships for each of the flights. Above-cloud legs allowed one to image the entire STBL and thus yield a more complete view of the spatial structure of precipitation. Because the near-surface region was always seen by the radar,

reflectivity–rain-rate relationships for a given flight can be used to estimate the mean precipitation flux at the surface over the nearly 7 h during which the aircraft was in the study area, thus allowing much improved estimates of the role of drizzle during DYCOMS-II.

The use of two antennas also made dual-Doppler analyses possible. Thus in addition to revealing the amount of drizzle in the STBL, and its local structure, the radar also images the velocity field in the cloud—particularly in weakly or nonprecipitating regions where the Doppler signal is dominated by air motions rather than the fall speeds of drizzle drops, which can be of a similar magnitude. In regions where drizzle is heavier, a variety of techniques are available to separate the fall speed contribution from the air motion contribution to the Doppler velocity fields.

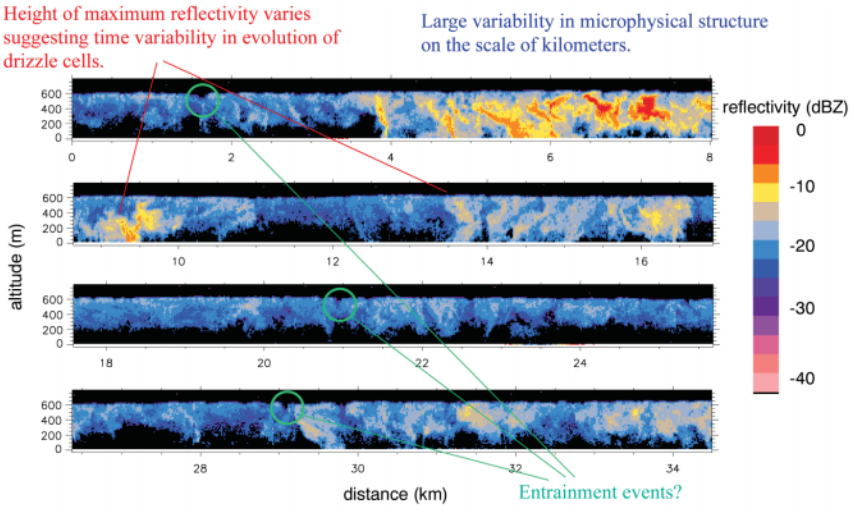

Fig. 5. Radar reflectivity for a segment of RF03. The axis scales are 1:1.

Two additional flights (RF06 and RF09) followed completely different patterns designed to evaluate the finescale structure and evolution of convective eddies within the cloud layer. Rather than large sweeping patterns designed to evaluate fluxes and budgets, RF06 and RF09 used staccato legs and sharp turns, which returned the aircraft to a selected point in the flow along a variety of headings (see electronic supplement DOI: 10.1175/BAMS-84-5-Stevens). This provides further insight into the interaction between microphysical and dynamical processes on the cloud scale, as well as a basis for comparing clouds observed during DYCOMS-II to those observed in previous campaigns (Vali et al. 1998) that used similar flight strategies.

As an example of the WCR data (Fig. 5) the structure of the cloud layer along a segment of RF03 shows considerable variability in reflectivity associated both with individual turbulent updrafts and downdrafts a few hundred meters wide and with mesoscale modulation on scales of 5 km or more. The variability in this 5-min flight segment foreshadows the variability among flights. Some flights sampled much more drizzle than this, some almost none. One of the remarkable impressions left on the investigators was how the apparent uniformity of the cloud top viewed from above could mask enormous variations in the microphysical structure within the cloud layer.

Intra- and interflight variability is hinted at in Fig. 6, where averaged reflectivities are converted into rain-rate profiles using relationships from previous field campaigns (Vali et al. 1998). Along with the mean profiles, profiles from subsegments illustrate the variability within the layer. Combined with Fig. 5 a picture emerges whereby drizzle is clearly a convective, rather than a stratiform, process, with drizzle rates in localized regions being orders of magnitude larger than elsewhere in the cloud. Layer-averaged drizzle rates greater than 0.5 mm day^{-1} (which correspond to evaporation rates of about 15 W m^{-2}) begin to have significant effects on the layer-averaged energetics. Local drizzle fluxes, which can be as large as 20 mm day^{-1}, would be expected to dominate the dynamics of circulations in their vicinity. In these cases the data suggest that drizzle helps organize the flow in a manner that helps maintain the cloud layer in the presence of drizzle, as there is circumstantial evidence that these regions of intense drizzle are remarkably persistent.

CLOUD MICROSTRUCTURE. Beyond the elementary issue of simply quantifying the propensity of stratocumulus to drizzle, the question arises as to what underlying physical processes regulate drizzle fluxes to begin with. The characteristics of the cloud layers observed during DYCOMS-II can be compared to previous observations (e.g., Austin et al. 1995; Gerber 1996) by comparing cloud droplet number concentrations, *N*, and cloud thickness. Initial indications are that the clouds observed during DYCOMS-II are somewhat thicker than the clouds that have been observed in this geographic region in the past. Observed clouds (see electronic supplement

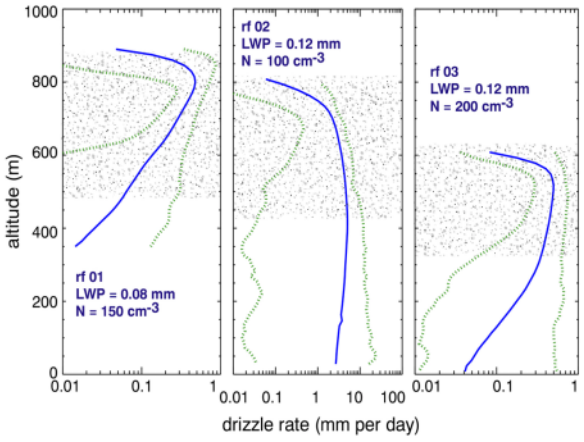

FIG. 6. Vertical profiles of precipitation rates estimated from the WCR data from RF01, RF02, and RF03. Stippled regions show the cloud layer. The blue lines are mean values for entire circles of about 200-km circumference. The dashed lines show the variability (90 %) for 1-km segments. The indicated liquid water paths (LWP) and droplet concentrations (N) are also mean values.

for a more detailed summary, DOI: 10.1175/BAMS-84-5-Stevens) ranged from less than 300 to over 500 m in depth, as compared to previous (mainly daytime) observations, where cloud depths tended to be between 150 and 300 m. While the cloud layers observed during DYCOMS-II had more cloud condensation nuclei (CCN) than some of the drizzling layers observed during studies elsewhere (e.g., the Atlantic Stratocumulus Transition Experiment), they were clearly characteristic of maritime clouds, with concentrations ranging from less than 100 to around 300 cm^{-3}.

Although the cloud microstructure is thought to influence, and in turn be influenced by, drizzle, might it not also tell us something about entrainment? Our discussion of entrainment above focused exclusively on entrainment rates, but what about entrainment processes—about which even less is known. The mixing of free-tropospheric air into the boundary layer requires warm, dry air parcels to mix with cool, saturated air parcels. Because warming and drying tend to evaporate cloud water, the detailed cloud microphysical structure can serve as an excellent indicator of mixing processes at cloud top. However, in this case one is likely to be less interested in average droplet concentrations or liquid water contents than in the details of the deviations from these averages. To investigate such details from the C130 requires instrumentation capable of sampling the flow at a very high rate.

To address these issues an ultrafast thermometer (UFT; Haman et al. 1997), a fast forward scattering spectrometer probe (FFSSP; Brenguier et al. 1998) capable of estimating the droplet distribution, and a particle volume monitor (PVM; Gerber 1994) for estimating liquid water were mounted within 6 m of each other (see electronic supplement DOI: 10.1175/BAMS-84-5-Stevens and Fig. S4) on the left wing of the C130. These probes all sampled the flow at rates of 1000 Hz or greater, thereby allowing one to explore the microphysical and thermodynamic structure of the cloud layer on scales ranging from 10 cm to several meters. It is expected that the data from these instruments will provide a first look at the smallest scales and the microphysical changes associated with the entrainment process at cloud top (see, e.g., Fig. 7).

THE AEROSOL. One aspect of the drizzle puzzle that human activities are known to influence is the background atmospheric aerosol, which regulates cloud droplet concentrations (N) and the average cloud microstructure. Largely for this reason, increasing attention is being given to quantifying relationships between the aerosol and stratocumulus microphysics. Some general rules regarding the relationship

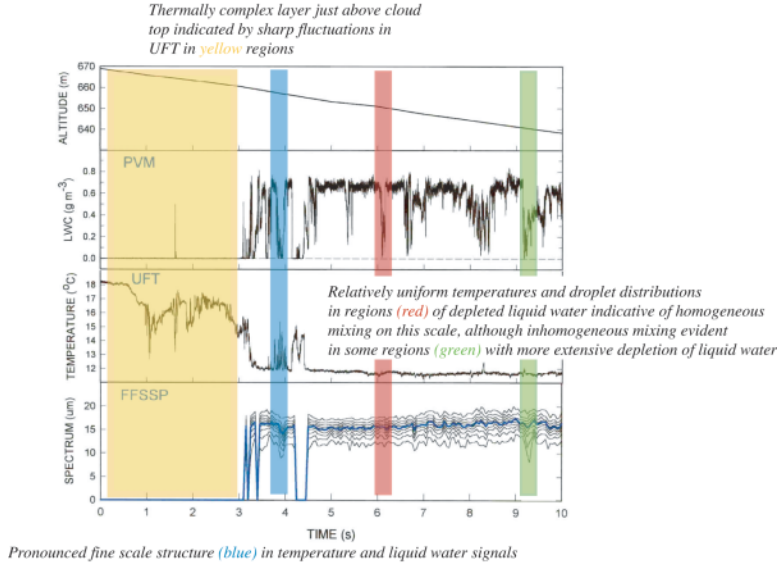

FIG. 7. Comparison of PVM, UFT, and FFSSP ultra-high-rate measurements during the flight of the NSF/NCAR C130 through the top of an unbroken layer of stratocumulus on 12 Jul (start of the 10-s interval is 12:05:38 UTC).

between aerosol properties (e.g., CCN or accumulation mode aerosol concentrations) and N (Erlick et al. 2001) and to some extent drizzle formation (e.g., the review by Schwartz and Slingo 1996) have been reported, but a comprehensive, physically based description of the aerosol and its impact on cloud microphysical processes remains outstanding.

Evaluations of the relationship between the CCN and N, by integrating parcel models over trajectory ensembles (e.g., Snider and Brenguier 2000), reveal consistency between predicted and observed values of N, but that agreement may reflect compensating biases in the measurements of vertical velocity, CCN, or N. The redundancy of the DYCOMS-II measurements of vertical velocity (C130 gust probe and possibly Doppler velocities from the WCR), two independent estimates of CCN spectra, and two estimates of N [from the scattering spectrometer probe (SPP-100) and the FFSPP-100)] should provide a more definitive test. Reflectivity measurements from the WCR are also providing an improved method for selecting nonprecipitation cloud regions for conducting these types of analyses.

Assuming consistency between the CCN and N can be established, attention can be focused on what is thought to be the more vexing problem (cf. Fig. 8)—

SECONDARY DYCOMS-II OBJECTIVES

The basic scientific objectives, and in particular the seven entrainment flights, also permitted a number of secondary objectives as highlighted below.

NIGHTTIME REMOTE SENSING. The DYCOMS-II program has provided a unique opportunity for evaluating and improving nighttime satellite remote sensing techniques, when the commonly used shortwave reflectance information is not available and while radiative forcing is controlled by thermal processes. The effects of nocturnal longwave cooling on cloud physics and dynamics also play an important role in the subsequent impacts of solar heating during the day. Little research has been conducted on nighttime multispectral satellite analysis techniques, and refinement of these methods could provide significant input to mesoscale forecasting methods. Due to the reduced information content of satellite observations at night, it is imperative that mesoscale model diagnostic and prognostic products be optimally combined with the remote sensing data. Field studies such as DYCOMS-II are thus needed for development of multicomponent data assimilation methods. Both geostationary and polar-orbiting satellite platforms were utilized to obtain research data for DYCOMS-II. The National Oceanic and Atmospheric Administration (NOAA) Geostationary Operational Environmental Satellite (GOES) is an essential source of information for determining temporal evolution of oceanic stratocumulus. Design improvements and better data distribution for geostationary satellite systems are making global near-continuous observations a reality, so that analysis techniques developed from DYCOMS will be applicable to other regions of persistent stratocumulus. New polar-orbiter satellites such as the National Aeronautics and Space Administration (NASA) *Terra* platform have less frequent time sampling, but provide higher spatial and spectral resolution that will aid in detailed testing of retrieval methods. The 15-min temporal resolution of GOES-West satellite data is being utilized for interpretation of cloud field evolution as the C130 aircraft flight circles moved with the wind field. Important aspects of these data include the identification of mesoscale dynamic processes and aerosol effects on microphysical characteristics.

FORECAST MODEL EVALUATION. Data collected during DYCOMS-II provide a natural basis for evaluating forecast products. Toward this end European Centre for Medium-Range Weather Forecasts (ECMWF) and National Centers for Environmental Prediction (NCEP) [Aviation Model (AVN)] model forecast calculations were archived for the entire month of July. Similarly, the U.S. Navy's Coupled Ocean/Atmosphere Mesoscale Prediction System (COAMPS) model was run with a relatively fine (6 km) nested mesh centered on the target area. Output, and the initial data for these calculations, were archived to allow subsequent sensitivity studies—with particular foci being the varying roles of model physics (especially microphysics) versus initialization on forecast quality. These data, when combined with archived remotely sensed data, in situ field data, and data of opportunity from buoys, ships, and soundings define a small mesoscale network that will be invaluable in evaluating forecast bias from various models. Of particular note in this regard is that because of logistical constraints on night flying, flights during the DYCOMS-II field phase were not chosen based on meteorology. In addition the region of flight operations is largely dictated by controls on airspace and air traffic lanes through restricted areas. Thus the flights are almost a random sample of conditions observed during the month.

specifically, how to relate the measured characteristics of the aerosol to the CCN, or alternatively *N*. Although the theory of Köhler (e.g., Rogers and Yau 1989) links aerosol and cloud properties, its application is complicated by the difficulty in properly accounting for the complexity of actual aerosol composition or the competing effects of particles in polluted conditions (Bigg 1986; Russell et al. 1999; Charlson et al. 2001). Most recently investigators from the second Aerosol Characterization Experiment (ACE-2) have documented discrepancies of up to a factor of 2 between the concentration calculated following the Köhler theory and CCN measurements (Raes et al. 2000; Brenguier et al. 2000a). One source for observed discrepancies could be sizing biases in the measurements. Bias in the CCN spectrum might result from overestimates of the applied supersaturation in the CCN chamber. For the aerosol spectrum, sizing biases could result from interpreting the measurements of morphologically complex particles as if they had been ideal, homogeneous spheres. An alternative hypothesis is that chemical components, such as organic compounds, are altering the surface tension, solubility, and water uptake due to mixture nonidealities neglected by the classical theory. DYCOMS-II provided the opportunity to address possible sizing biases or compositional effect with complementary techniques.

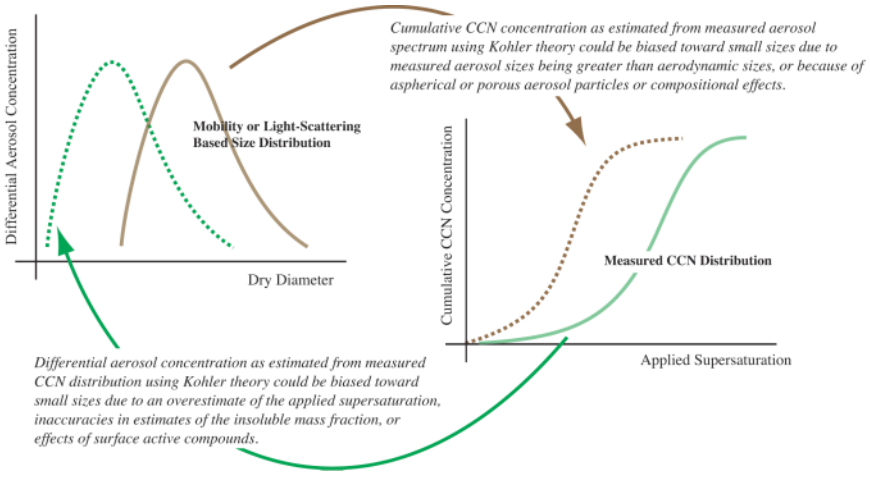

Fig. 8. Illustration of the relationship between the dry aerosol size spectrum and the CCN distribution, and the problems that can occur in attempting to relate one to the other.

Sizing biases in the aerosol spectrum as measured during DYCOMS-II are being evaluated in a number of ways. First, the size distribution is a blending of data from a variety of instruments, that is, a scattering spectrometer probe (SPP-300) measures particles of 0.3–20-μm diameter, a passive cavity aerosol spectrometer (SPP-200) measures particles of 0.1–0.3-μm diameter, and a radial differential mobility analyzer (RDMA) measures particles of 0.01–0.1-μm diameter (see the electronic supplement for a more complete description of the particle-sizing probes DOI: 10.1175/BAMS-84-5-Stevens). These measurements are being compared to redundant condensation nuclei counters (which measure the total aerosol concentration). Second, in situ estimates of the aerosol size distribution are being compared to distributions derived from microscopic sizing of the aerosol impacted on a filter. Last, a diffusion battery is being used to compare size-segregated measurements of CCN and total aerosol concentrations (e.g., Gras 1990).

Composition effects on the activation spectrum of the aerosol spectrum are also investigated using DYCOMS-II data. The composition of the subcloud aerosol is being determined from an analysis of individual particles as well as from bulk samples collected on filters during subcloud flight legs. Electron microscopy (e.g., Pósfai et al. 1999) of individual aerosol particles provides qualitative information on elemental composition, complemented by bulk filter analysis using X-ray fluorescence for elements and Fourier transform infrared spectroscopy for functional groups—thus providing an opportunity to examine both external mixing of different types of particles and the role of organics (Maria et al. 2002). To better understand the detailed composition of that component of the subcloud aerosol that is actually activated into cloud droplets, a counterflow virtual impactor (Twohy et al. 2001) was flown during DYCOMS-II to collect individual droplet residual particles after evaporation. These residual particles are being analyzed similarly to the subcloud aerosol. Additional compositional information is provided by an experimental cloud water collector (Straub et al. 2001), which allows the quantification of pH, inorganic ions, and total organic carbon in cloud droplets residing at different levels in the cloud. These latter techniques, which look at the composition of cloud droplets, can also lend insight into the modification of aerosol composition through repeated cycles of activation and evaporation of cloud droplets.

SUMMARY AND SPECULATION. A recent field program, DYCOMS-II, was conducted in the stratocumulus regime of the northeast Pacific. In roughly descending order of emphasis DYCOMS-II strove to answer four questions: (i) What is the entrainment rate? (ii) How much does it drizzle? (iii) What is the nature of cloud microphysical variability on submeter scales? (iv) Can the activation spectrum of cloud droplets be understood based on measurements of the atmospheric aerosol?

To answer these questions DYCOMS-II made use of novel instrumentation and flight strategies. These included nocturnal flights, which integrated remote sensing (cloud radar, lidar, radiometers, and dropsondes) and in situ data collection (using standard turbulence and thermodynamic probes as well as an enhanced suite of microphysical instrumentation) from a single airborne platform. In addition a new method for making fast measurements of atmospheric dimethyl sulfide (DMS) was employed to study entrainment mixing. Overall DYCOMS-II brought together a large suite of instrumentation capable of describing the dynamics, chemistry, and physics of the stratocumulus-topped boundary layer over an unprecedented range of scales. DYCOMS-II also benefited from the good fortune of extraordinarily cooperative meteorology; conditions were ideal on every flight. Such a combination of favorable meteorology and extensive instrumentation can be expected to produce as many surprises as answers. In this respect some puzzles to emerge from initial analyses of the data include the origins of remarkably large variability in boundary layer DMS, and mechanisms for sustaining persistent regions of very strong drizzle.

In addition to the emerging puzzles, in closing it also seems fitting to outline at least some of the preliminary findings that are being explored with great interest—even if so doing involves some degree of extrapolation from the data presented above. Broadly speaking, the finding with perhaps the widest implications is that stratocumulus appears to entrain less and drizzle more than previously thought. For instance, during RF01 (see Fig. 2) the cloud-top interface was unstable by many measures, yet the cloud appeared to thicken substantially during the course of the flight. Preliminary analyses also indicate a remarkable degree of correspondence among various tracer-based estimates of entrainment, all of which produce entrainment rates of order 0.4 cm s^{-1}, which is significantly smaller than what is predicted by many current parameterizations. Indeed preliminary attempts to apply parameterized entrainment relations to the observed cloud layers generally result in a marked thinning of the layer.

The extent of drizzle observed during DYCOMS-II is consistent with entrainment drying of the cloud layer being rather inefficient, but is nonetheless remarkable. On some flights preliminary estimates of drizzle rates at the surface over large areas and long time periods averaged near a millimeter per day. Even on flights where relatively little drizzle reached the surface, drizzle fluxes at cloud base could be pronounced. Indeed, the canonical picture of "nonprecipitating marine stratocumulus" was rather more rare than common, suggesting that drizzle might indeed be a key element of the dynamics of the STBL. Although conclusions such as the above are necessarily speculative they do provide the promise that the DYCOMS-II data will teach us fundamentally new things and, thus, whet the appetite for further investigation.

ACKNOWLEDGMENTS. DYCOMS-II is in many ways the first experiment of the GCSS project, as it is a direct outgrowth of this endeavor's activities. DYCOMS-II was made possible partly with the support of the Alexander von Humboldt Foundation, who supported the first author during the planning phase. Support for the project itself was provided by NSF Grant ATM-0097053, which was made possible because of the keen interest, involvement, and encouragement of both Roddy Rogers of NSF and Dave Carlson of NCAR. We appreciate the assistance of Anton Beljaars, Martin Köhler, Steve Krueger, and Hua-Lu Pan for making column data (from ECMWF and NCEP, respectively) available to DYCOMS-II investigators. We thank William R. Thompson for making COAMPS data available on a fine grid centered on the experiment target area, Slobodan Jovcic for writing the Web-based mission summary software used during the flights, and Jim John (of North Island Naval Air Station) for his help in coordinating our use of the naval air station. We would also like to acknowledge the support of Jim Anderson, Phil Austin, Henry Boynton, Graham Feingold, Bruce Gandrud, Bart Geerts, Krystof Haman, Yefim Kogan, Errol Korn, Dave Leon, David Mechem, Glenn Mitchell, James Murakami, Monica Rivera, Steve Roberts, Ron Ruth, Jeff Stith, Bozena Strus, Qing Wang, Shouping Wang, Chris Webster, the engineers, programmers, management, pilots, mechanics, and scientists of the Research Aviation Facility, and the staff of North Island Naval Air Station. Some of these individuals are worthy of author status, but chose to forgo it. Lynn Russell acknowledges support from NASA Grant NAG5-8676. Research by Chai, Szumowski, and Wetzel was supported by ONR Grants N00014-01-1-0295 and N00014-01-1-0663. Data available online from www.joss.ucar.edu/dycoms.

APPENDIX: DATA. Because of the enormous amount of data collected during DYCOMS-II, much of it from instruments developed and operated by individual investigators, an important component of the experimental strategy is the development of a proper archive. This is even more pressing when one considers the amount of relevant data available from space-based platforms, the subjective opinions of on-site observers, and other sources of opportunity. To identify and collect data in the latter category, investigators worked with the Joint Office for Scientific Support (JOSS, which operates as part of the University Corporation for Atmospheric Research) to develop an online field catalog, which provided centralized access to information and data relating to all aspects of the field operations. This catalog included various textual reports (e.g., weather forecasts and aircraft flight summaries); a number of imagery products that were either produced by JOSS (e.g., high-resolution satellite images and loops), produced by DYCOMS-II scientists (e.g., specialized model products), or gathered from various Internet sources (e.g., oceanographic analyses from the Naval Oceanographic Office); and finally information on each of the aircraft missions (e.g., takeoff and landing times, flight tracks, dropsonde data, etc.). The catalog was used in the field for operations and planning support as well as allowing scientists not in the field to follow the progress of the project. It was also a useful tool after the completion of the field phase to help determine cases for analysis.

After the field phase the field catalog was blended with other sources of data not available in real time (ranging from aircraft data to satellite radiances) to form the DYCOMS-II data archive. This archive provides distributed access to all of the operational and research datasets collected during the project. It will continue to grow as various processed products are added to it. For instance simulations that attempt to synthesize the observed cases may later be incorporated into the archive. Both the catalog and the archive are available to all via the DYCOMS-II Data Management Web page (www.joss.ucar.edu/dycoms). They provide a natural starting point for researchers interested in DYCOMS-II datasets, which we hope will be extensively used.

REFERENCES

Ackerman, A. S., O. B. Toon, and P. V. Hobbs, 1993: Dissipation of marine stratiform cloud and collapse of the marine boundary layer due to the depletion of cloud condensation nuclei by clouds. *Science,* **262,** 226–229.

Albrecht, B. A., 1989: Aerosols, cloud microphysics and fractional cloudiness. *Science,* **245,** 1227–1230.

——, D. A. Randall, and S. Nicholls, 1988: Observations of marine stratcumulus clouds during FIRE. *Bull. Amer. Meteor. Soc.,* **69,** 618–626.

——, C. S. Bretherton, D. Johnson, W. S. Schubert, and A. S. Frisch, 1995: The Atlantic Stratocumulus Transition Experiment—ASTEX. *Bull. Amer. Meteor. Soc.,* **76,** 889–904.

Austin, P., Y. Wang, R. Pincus, and V. Kujala, 1995: Precipitation in stratocumulus clouds: Observational and modeling results. *J. Atmos. Sci.,* **52,** 2329–2352.

Bigg, E. K., 1986: Discrepancy between observation and prediction of concentrations of cloud condensation nuclei. *Atmos. Res.,* **20,** 82–86.

Brenguier, J.-L., T. Bourrianne, A. de Araujo Coelho, R. J. Isbert, R. Peytavi, D. Trevarin, and P. Weschler, 1998: Improvements of droplet distribution size meaurements with the Fast-FSSP (Forward Scattering Spectrometer Probe). *J. Atmos. Oceanic Technol.,* **15,** 1077–1090.

——, and Coauthors, 2000a: An overview of the ACE-2 CLOUDYCOLUMN closure experiments. *Tellus,* **52B,** 814–826.

——, H. Pawlowska, L. Schuüller, R. Preusker, J. Fischer, and Y. Fouquart, 2000b: Radiative properties of boundary layer clouds: Droplet effective radius versus number concentration. *J. Atmos. Sci.,* **57,** 803–821.

Bretherton, C. S., P. Austin, and S. T. Siems, 1995: Cloudiness and marine boundary layer dynamics in the ASTEX Lagrangian experiments. Part II: Cloudiness, drizzle, surface fluxes, and entrainment. *J. Atmos. Sci.,* **52,** 2724–2735.

Brost, R. A., J. C. Wyngaard, and D. H. Lenschow, 1982: Marine stratocumulus layers. Part II: Turbulence budgets. *J. Atmos. Sci.,* **39,** 818–836.

Charlson, R. J., J. H. Seinfeld, A. Nenes, M. Kulmala, A. Laaksonen, and M. C. Facchini, 2001: Atmospheric science—Reshaping the theory of cloud formation. *Science,* **292,** 2025–2026.

Chen, C., and W. R. Cotton, 1987: The physics of the marine statocumulus-capped mixed layer. *J. Atmos. Sci.,* **44,** 2951–2977.

Deardorff, J. W., 1972: Parameterization of the planetary boundary layer for use in general circulation models. *Mon. Wea. Rev.,* **100,** 93–106.

DeRoode, S. R., and P. G. Duynkerke, 1997: Observed Lagrangian transition of stratocumulus into cumulus during ASTEX: Mean state and turbulence structure. *J. Atmos. Sci.,* **54,** 2157–2173.

Duynkerke, P. G., H. Zhang, and P. J. Jonker, 1995: Microphysical and turbulent structure of nocturnal stra-

tocumulus as observed during ASTEX. *J. Atmos. Sci.,* **52,** 2763–2777.

Erlick, C., L. M. Russell, and V. Ramaswamy, 2001: Microphysics-based investigation of the radiative effects of aerosol–cloud interactions for two MAST experiment case studies. *J. Geophys. Res.,* **106,** 1249–1270.

Fox, N. I., and A. J. Illingworth, 1997: The retrieval of stratocumulus cloud properties by ground-based cloud radar. *J. Appl. Meteor.,* **36,** 485–492.

Gerber, H., 1994: New microphysics sensor for aircraft use. *Atmos. Res.,* **31,** 235–252.

——, 1996: Microphysics of marine stratocumulus clouds with two drizzle modes. *J. Atmos. Sci.,* **53,** 1649–1662.

Gras, J., 1990: Cloud condensation nuclei over the southern ocean. *Geophys. Res. Lett.,* **17,** 1565–1567.

Haman, K. E., A. Makulski, and S. P. Malinowski, 1997: A new ultrafast thermometer for airborne measurements in clouds. *J. Atmos. Oceanic Technol.,* **14,** 217–227.

Kawa, S. R., and R. Pearson Jr., 1989: An observational study of stratocumulus entrainment and thermodynamics. *J. Atmos. Sci.,* **46,** 2649–2661.

Lenschow, D. H., 1996: A proposal for measuring entrainment into the cloud-capped boundary layer. *Proc. ETL/CSU Cloud-Related Process Modeling and Measurement Workshop,* Boulder, CO, NOAA/ETL, 29–55.

——, and Coauthors, 1988: Dynamics and Chemistry of Marine Stratocumulus (DYCOMS) experiment. *Bull. Amer. Meteor. Soc.,* **69,** 1058–1067.

——, P. B. Krummel, and S. T. Siems, 1999: Measuring entrainment, divergence, and vorticity on the mesoscale from aircraft. *J. Atmos. Oceanic Technol.,* **16,** 1384–1400.

Lilly, D. K., 1968: Models of cloud topped mixed layers under a strong inversion. *Quart. J. Roy. Meteor. Soc.,* **94,** 292–309.

Liu, W. T., 2002: Progress in scatterometer application. *J. Oceanogr.,* **58,** 121–136.

Ma, C.-C., C. R. Mechoso, A. W. Robertson, and A. Arakawa, 1996: Peruvain stratus clouds and the tropical Pacific circulation. *J. Climate,* **9,** 1635–1645.

Maria, S. F., L. M. Russell, B. J. Turpin, and R. Porcja, 2002: FTIR measurements of functional groups and organic mass in aerosol samples over the Caribbean. *Atmos. Environ.,* **36,** 5185–5196.

May, R. D., 1998: Open-path, near-infrared tunable diode laser spectrometer for atmospheric measurements of H_2O. *J. Geophys. Res.,* **103,** 19 161–19 172.

Mechoso, C. R., and Coauthors, 1995: The seasonal cycle over the tropical Pacific in coupled ocean–atmosphere general circulation models. *Mon. Wea. Rev.,* **123,** 2825–2838.

Moeng, C.-H., and Coauthors, 1996: Simulation of a stratocumulus-topped PBL: Intercomparison among different numerical codes. *Bull. Amer. Meteor. Soc.,* **77,** 261–278.

Nicholls, S., 1984: The dynamics of stratocumulus: Aircraft observations and comparisons with a mixed layer model. *Quart. J. Roy. Meteor. Soc.,* **110,** 783–820.

Paluch, I. R., and D. H. Lenschow, 1991: Stratiform cloud formation in the marine boundary layer. *J. Atmos. Sci.,* **48,** 2141–2157.

Philander, S. G. H., D. Gu, D. Halpern, G. Lambert, N.-C. Lau, T. Li, and R. Pacanowski, 1996: Why the ITCZ is mostly north of the equator? *J. Climate,* **9,** 2958–2972.

Pincus, R., and M. B. Baker, 1994: Effect of precipitation on the albedo susceptibility of marine boundary layer clouds. *Nature,* **372,** 250–252.

Pósfai, M., J. Anderson, P. R. Buseck, and H. Sievering, 1999: Soot and sulfate aerosol particles in the remote marine troposphere. *J. Geophys. Res.,* **104,** 21 685–21 693.

Raes, F., T. Bates, F. McGovern, and M. van Liedekerke, 2000: The Second Aerosol Characterization Experiment (ACE-2): General overview and main results. *Tellus,* **52B,** 111–125.

Rodwell, M. J., and B. J. Hoskins, 2001: Subtropical anticyclones and summer monsoons. *J. Climate,* **14,** 3192–3211.

Rogers, R. R., and M. K. Yau, 1989: *A Short Course in Cloud Physics.* 3d ed. International Series in Natural Philosophy, Butterworth Heinemann, 290 pp.

Russell, L. M., and Coauthors, 1999: Aerosol dynamics in ship tracks. *J. Geophys. Res.,* **104,** 31 077–31 096.

Schwartz, S. E., and A. Slingo, 1996: Enhanced shortwave cloud radiative forcing due to anthropogenic aerosols. *Clouds, Chemistry and Climate,* P. J. Crutzen and V. Ramanathan, Eds., Springer-Verlag, 191–236.

Snider, J. R., and J.-L. Brenguier, 2000: A comparison of cloud condensation nuclei and cloud droplet measurements obtained during ACE-2. *Tellus,* **52B,** 828–842.

Stephens, G. L., and T. J. Greenwald, 1991: The Earth's radiation budget and its relation to atmospheric hydrology. 2. Observations of cloud effects. *J. Geophys. Res.,* **96,** 15 325–15 340.

Stevens, B., 2002: Entrainment in stratocumulus mixed layers. *Quart. J. Roy. Meteor. Soc.,* **128,** 2663–2690.

——, W. R. Cotton, G. Feingold, and C.-H. Moeng, 1998: Large-eddy simulations of strongly precipitating, shallow, stratocumulus-topped boundary layers. *J. Atmos. Sci.,* **55,** 3616–3638.

——, C.-H. Moeng, and P. P. Sullivan, 1999: Large-eddy simulations of radiatively driven convetion: Sensitivities to the representation of small scales. *J. Atmos. Sci.,* **56,** 3963–3984.

Straub, D., J. L. Collett Jr., D. Baumgardner, and R. Friesen, 2001: Design and characterization of a new airborne cloud water sampler. *Proc. Second Int. Conf. on Fog and Fog Collection,* St. John's, NF, Canadian International Development Agency, Environment Canada, Meteorological Service of Canada, International Development Research Centre, Canadian Meteorological and Oceanographic Society, Government of Newfoundland and Labrador, Molson Canada, Rodrigues Winery, Newfoundland and Labrador Development Corporation, 209–212.

Twohy, C. H., J. G. Hudson, S. S. Yum, J. R. Anderson, S. K. Durlak, and D. Baumgardner, 2001: Characteristics of cloud nucleating aerosols in the Indian Ocean region. *J. Geophys. Res.,* **106,** 28 699–28 710.

Twomey, S. A., 1974: Pollution and the planetary albedo. *Atmos. Environ.,* **8,** 1251–1256.

Vali, G., R. D. Kelly, J. French, S. Haimov, D. Leon, R. E. McIntosh, and A. Pazmany, 1998: Finescale structure and microphysics of coastal stratus. *J. Atmos. Sci.,* **55,** 3540–3564.

Wang, S., and B. A. Albrecht, 1986: A stratocumulus model with an internal circulation. *J. Atmos. Sci.,* **43,** 2374–2390.

——, and Q. Wang, 1994: Roles of drizzle in a one-dimensional third-order turbulence closure model of the nocturnal stratus-topped marine boundary layer. *J. Atmos. Sci.,* **51,** 1559–1576.